COMPDYN 2013
4th ECCOMAS Thematic Conference on
Computational Methods in Structural Dynamics and Earthquake Engineering
M. Papadrakakis, V. Papadopoulos, V. Plevris (eds.)
Kos Island, Greece, 12–14 June 2013

APPLICATIONS OF VARIATIONALLY CONSISTENT SELECTIVE MASS SCALING IN EXPLICIT DYNAMICS

Anton Tkachuk[1], **Manfred Bischoff**

[1] Institute of Structural Mechanics, University of Stuttgart
Pfaffenwaldring 7, 70569 Stuttgart, Germany
e-mail: {tkachuk,bischoff}@ibb.uni-stuttgart.de

Keywords: Selective mass scaling, Hamilton's principle, explicit dynamics, hybrid-mixed.

Abstract. *The aim of Selective Mass Scaling (SMS) in context of non-linear structural mechanics is to increase the critical time-step for explicit time integration without substantial loss in accuracy in the lower modes. The Conventional Mass Scaling (CMS) adds artificial mass only to diagonal terms of the lumped mass matrix and thus preserves diagonal format of mass matrix. It is usually applied in little number of small or stiff elements, like spot-welds in car crash, whose high eigenfrequencies limit time-step. However, translational and rotational inertia of the structure increases, which may cause non-physical phenomena. SMS technique adds artificial terms both to diagonal and non-diagonal terms, which results in non-diagonal mass matrix, but at least allows preservation of translational mass. Thus SMS can be used uniformly in domain with less non-physical artifacts. The previous works on SMS rely on algebraically constructed mass scaling matrices or stiffness proportional mass scaling. These approaches provide very small choice of mass scaling templates and they lack rigorous variational formulation. The goal of this paper is to develop variational basis for SMS with consistent discretization of inertial term and to assess efficiency of the proposed approach.*

1 INTRODUCTION

Scaling of inertia for explicit time integration is a common procedure since 70s. For beam and shell elements diagonal terms of rotational inertia are scaled using formulas given in [6, 2]. This allows to increase the critical step of these elements up to corresponding critical step of rod or membrane element. The Conventional Mass Scaling for translational degrees of freedom is described in manuals of *LS-Dyna*, *Radioss* etc. Application of CMS is limited to little number of small or stiff elements with overall increase of mass of model up to 1-3%.

Selective mass scaling was proposed by group of Lars Olovsson [8, 10] and it aimed increasing of stable time-step for explicit integration of solid-based shells and eight-node hexahedral elements. In combination with an iterative solver for acceleration (see [9]) it proved to be efficient for some applications such as deep drawing of metal sheets and drop tests [3], dynamics of solid-shell modeled structures [4].

The original idea of paper [10] relies on following *algebraic* construction of scaled mass matrix of individual element $\mathbf{m}^\circ$

$$\begin{aligned} \mathbf{m}^\circ &= \mathbf{m}_e + \boldsymbol{\lambda}^\circ \\ \boldsymbol{\lambda}^\circ &= \triangle m \left(\mathbf{I} - \sum_i \mathbf{e}_i^T \mathbf{e}_i \right) \end{aligned} \tag{1}$$

where $\mathbf{m}_e$ and $\boldsymbol{\lambda}^\circ$ are lumped mass matrix (LMM) and mass augmentation (MA), $\triangle m$ is artificially added mass and $\mathbf{e}_i$ is some set of *rigid body modes*. Initially it was proposed to include only translational rigid body modes [10]. Later implementation also included rigid body rotation [3]. Hence, the properties of the algebraic SMS are defined by linear hull of vectors $\mathbf{e}_i$.

SMS has following effect on structural behavior. The critical time-step roughly increases by factor $\sqrt{1+\beta}$ with β being ratio of added mass to element mass $\triangle m/m$, see [9]. The eigenmodes of the structure are distorted and the order of the modes is changed. If only translational rigid body modes are taken then rotary inertia of the structure is excessive. If all rigid body modes are taken then the rotary inertia is preserved, but the scaled mass matrix obtains coupled terms between inertia in x-, y- and z-directions [3]. Condition number of the global mass matrix $\mathbf{M}^\circ$ increases by factor approximately $1+2\beta$ and number of iterations needed for solution of the system $\mathbf{Ma} = \mathbf{f}$ grows proportionally to $\sqrt{1+2\beta}$.

Variationally based method for SMS was proposed recently in [11]. The starting point of the proposed approach is a new parametrized variational principle of elasto-dynamics, which can be interpreted as penalized Hamiltons principle. It uses independent variables for displacement, velocity and momentum (three-field formulation). The penalized Hamiltons principle imposes relations between velocity, momenta and displacements via penalty method. Consistent discretization of the latter principle results in a parametric family of mass matrices. In this way the translational inertia, center of gravity and polar momenta of individual elements may be preserved, which guarantees convergence of the method with mesh refinement. Thus, the distinctive feature of the method is variational rigorousness, mass augmentation is prescribed via ansatz spaces and more accurate results for bending dominated problems can be obtained.

Variational mass scaling in paper [11] considered general three-field formulation for linear elasto-dynamics and only three-node triangle, four-node quadrilateral and eight-node hexahedral elements. Here, variational mass scaling based on simplified two-field formulation is discussed. The examples are focused on nine-node and eight-node quadrilateral elements. For the eight-node quadrilateral element no good LMM is available [12, 7], which makes SMS for the

element very promising. Results for transient and eigenfrequency benchmarks are given and discussed.

2 TWO-FIELD VARIATIONAL FORMULATION OF ELASTO-DYNAMICS

In this section the modified variational formulation is derived. Consider the strong form of initial value problem for finite strain dynamics

$$\begin{cases} \rho_0 \ddot{\mathbf{u}} = \mathrm{DIV}\,\mathbf{P} + \rho_0 \hat{\mathbf{b}} & \text{in } (0, t_{\mathrm{end}}] \times \mathcal{B} \\ \mathbf{F} = \mathbf{I} + \dfrac{\partial \mathbf{u}}{\partial \mathbf{X}} & \text{in } (0, t_{\mathrm{end}}] \times \mathcal{B} \\ \mathbf{P} = \mathbf{P}(\mathbf{F}) & \text{in } (0, t_{\mathrm{end}}] \times \mathcal{B} \\ \mathbf{u}(t=0) = \mathbf{u}_0 & \text{in } \mathcal{B} \\ \dot{\mathbf{u}}(t=0) = \mathbf{v}_0 & \text{in } \mathcal{B} \\ \mathbf{u} = \mathbf{0} & \text{in } (0, t_{\mathrm{end}}] \times \partial\mathcal{B}_u \\ \mathbf{P}\mathbf{n} = \hat{\mathbf{t}} & \text{in } (0, t_{\mathrm{end}}] \times \partial\mathcal{B}_\sigma, \end{cases} \tag{2}$$

where $\mathbf{u}$ and $\mathbf{F}$ are displacements vector and deformation gradient, $\mathbf{P}$ is 1^{st} Piola-Kirchhoff stress tensor, which can be found from a given constitutive equation $\mathbf{P}(\mathbf{F})$, ρ_0 and $\hat{\mathbf{b}}$ are an initial material density and a body load, respectively, $\mathbf{u}_0$ and $\mathbf{v}_0$ are initial displacement and velocity, $\partial\mathcal{B}_u$ is part of surface with prescribed zero displacement and $\hat{\mathbf{t}}$ is prescribed traction on part of surface $\partial\mathcal{B}_\sigma$. The problem is stated with respect to the actual configuration of the body $\mathcal{B}$ within a given time interval $(0, t_{\mathrm{end}}]$.

Following the standard derivation (see [2]), the virtual work principle can be written as

$$\begin{aligned} &\delta W^{\mathrm{int}}(\mathbf{u}, \delta u) - \delta W^{\mathrm{ext}}(\mathbf{u}, \delta u) + \delta W^{\mathrm{kin}}(\mathbf{u}, \delta u) = 0 \\ &\delta W^{\mathrm{int}}(\mathbf{u}, \delta u) = \int_{\mathcal{B}_0} \delta\mathbf{F} : \mathbf{P}\,\mathrm{d}V \\ &\delta W^{\mathrm{ext}}(\mathbf{u}, \delta u) = \int_{\mathcal{B}_0} \delta\mathbf{u} \cdot \rho_0 \hat{\mathbf{b}}\,\mathrm{d}V + \int_{\partial\mathcal{B}_{\sigma,0}} \delta\mathbf{u} \cdot \hat{\mathbf{t}}\,\mathrm{d}A \\ &\delta W^{\mathrm{kin}}(\mathbf{u}, \delta u) = \int_{\mathcal{B}_0} \delta\mathbf{u} \cdot \rho_0 \ddot{\mathbf{u}}\,\mathrm{d}V, \end{aligned} \tag{3}$$

where $\delta\mathbf{u}$ is kinematically admissible displacement, $\mathcal{B}_0$ and $\partial\mathcal{B}_{\sigma,0}$ are reference domain and pull-back to reference configuration of traction boundary.

We propose to modify the weak statement(3) by introduction of independent variable for velocity $\mathbf{v}$. The kinematic equation between velocity and displacement $\dot{\mathbf{u}} = \mathbf{v}$ can be imposed weakly in modified expression for work of d'Alembert forces

$$\delta W^{\mathrm{kin},\circ}(\mathbf{u}, \delta\mathbf{u}, \mathbf{v}, \delta\mathbf{v}) = \int_{\mathcal{B}_0} \delta\mathbf{u} \cdot \left[(1 + C_1)\rho_0 \ddot{\mathbf{u}} - C_1 \dot{\mathbf{v}}\right]\,\mathrm{d}V - \int_{\mathcal{B}_0} \delta\mathbf{v} \cdot \left[\rho_0 C_1 (\dot{\mathbf{u}} - \mathbf{v})\right]\,\mathrm{d}V. \tag{4}$$

Here constant C_1 plays a role of penalty factor, see [11].

Substitution of the latter expression in (3) instead of δW^{kin} leads to formulation used herein. Note, that if internal and external forces possess potentials $\delta\Pi = \delta W^{\mathrm{int}} - \delta W^{\mathrm{ext}}$, then the

modified formulation is equivalent to penalized Hamiltonian formulation

$$\begin{aligned} \delta H^{\circ}(\mathbf{u},\mathbf{v}) &= \delta \int_0^{t_{\mathrm{end}}} (T^{\circ} - \Pi)\,\mathrm{d}t \\ T^{\circ} &= \int_{\mathcal{B}_0} \left[\frac{1}{2}\rho_0 \dot{\mathbf{u}}\cdot\dot{\mathbf{u}} + \frac{C_1}{2}\rho_0(\mathbf{v}-\dot{\mathbf{u}})\cdot(\mathbf{v}-\dot{\mathbf{u}})\right]\mathrm{d}V. \end{aligned} \tag{5}$$

3 DISCRETIZATION

Here a standard total Lagrangian formulation of weak form (3) with modified inertia term (4) is used. Displacements are discretized with time-independent shape function matrix $\mathbf{N}$. Shape functions for velocity field $\boldsymbol{\psi}$ may depend on time see for reasons Section 4. Thus, the approximations of fields reads as follows

$$\begin{aligned} \mathbf{u}^h &= \mathbf{N}\mathbf{U} & \mathbf{v}^h &= \boldsymbol{\psi}\mathbf{V} \\ \delta\mathbf{u}^h &= \mathbf{N}\delta\mathbf{U} & \delta\mathbf{v}^h &= \boldsymbol{\psi}\delta\mathbf{V} \\ \dot{\mathbf{u}}^h &= \mathbf{N}\dot{\mathbf{U}} & \dot{\mathbf{v}}^h &= \boldsymbol{\psi}\dot{\mathbf{V}} + \dot{\boldsymbol{\psi}}\mathbf{V} \\ \ddot{\mathbf{u}}^h &= \mathbf{N}\ddot{\mathbf{U}} \end{aligned} \tag{6}$$

Substitution of the latter ansatz in the virtual work expression yields

$$\begin{aligned} \delta W^{\mathrm{int},h} &= \delta\mathbf{U}^{\mathrm{T}} \int_{\mathcal{B}_0} \mathbf{B}^{\mathrm{T}}\mathbf{P}\,\mathrm{d}V = \delta\mathbf{U}^{\mathrm{T}}\mathbf{f}^{\mathrm{int}} \\ \delta W^{\mathrm{ext},h} &= \delta\mathbf{U}^{\mathrm{T}} \int_{\mathcal{B}_0} \mathbf{N}^{\mathrm{T}}\rho_0\hat{\mathbf{b}}\,\mathrm{d}V + \delta\mathbf{U}^{\mathrm{T}} \int_{\partial\mathcal{B}_{\sigma,0}} \mathbf{N}\hat{\mathbf{t}}\,\mathrm{d}A = \delta\mathbf{U}\mathbf{f}^{\mathrm{ext}} \\ \delta W^{\mathrm{kin},\circ,h} &= \delta\mathbf{U}^{\mathrm{T}} \int_{\mathcal{B}_0} \mathbf{N}^{\mathrm{T}}\left[(1+C_1)\rho_0\mathbf{N}\ddot{\mathbf{U}} - C_1(\boldsymbol{\psi}\dot{\mathbf{V}} - \dot{\boldsymbol{\psi}}\mathbf{V})\right]\mathrm{d}V - \\ &\quad \delta\mathbf{V}^{\mathrm{T}} \int_{\mathcal{B}_0} \boldsymbol{\psi}^{\mathrm{T}}\left[(1+C_1)\rho_0(\mathbf{N}\dot{\mathbf{U}} - \boldsymbol{\psi}\mathbf{V})\right]\mathrm{d}V = \\ &\quad \delta\mathbf{U}^{\mathrm{T}}\left[(1+C_1)\mathbf{M} - C_1\mathcal{A}\dot{\mathbf{V}} - C_1\dot{\mathcal{A}}\mathbf{V}\right] - C_1\delta\mathbf{V}^{\mathrm{T}}\left[\mathcal{A}^{\mathrm{T}}\dot{\mathbf{U}} - \mathcal{Y}\mathbf{V}\right], \end{aligned} \tag{7}$$

where $\mathbf{f}^{\mathrm{int}}$ and $\mathbf{f}^{\mathrm{ext}}$ are internal and external nodal force vectors, $\mathbf{M} = \int_{\mathcal{B}_0}\rho_0\mathbf{N}^{\mathrm{T}}\mathbf{N}\,\mathrm{d}V$ is CMM, $\mathcal{A} = \int_{\mathcal{B}_0}\rho_0\mathbf{N}^{\mathrm{T}}\boldsymbol{\psi}\,\mathrm{d}V$ is projection matrix $\mathbf{V}\to\mathbf{U}$ and $\mathcal{Y} = \int_{\mathcal{B}_0}\rho_0\boldsymbol{\psi}^{\mathrm{T}}\boldsymbol{\psi}\,\mathrm{d}V$ is a mass matrix computed for discrete velocity vector $\mathbf{V}$. For the actual motion the sum of the virtual work terms vanishes, thus leading to equations of motion with kinematic constrains

$$\begin{aligned} \left[(1+C_1)\mathbf{M}\ddot{\mathbf{U}} - C_1\mathcal{A}\dot{\mathbf{V}} - C_1\dot{\mathcal{A}}\mathbf{V}\right] + \mathbf{f}^{\mathrm{int}} &= \mathbf{f}^{\mathrm{ext}} \\ \mathcal{A}^{\mathrm{T}}\dot{\mathbf{U}} &= \mathcal{Y}\mathbf{V}. \end{aligned} \tag{8}$$

Elimination of vector $\mathbf{V}$ from equation (8_1) using equation (8_2) leads to final expression of equation of motion, scaled mass and mass augmentation

$$\begin{aligned} \mathbf{M}^{\circ}\ddot{\mathbf{U}} + \mathbf{f}^{\mathrm{int}} &= \mathbf{f}^{\mathrm{ext}} - \frac{\mathrm{d}\boldsymbol{\lambda}^{\circ}}{\mathrm{d}\,t}\dot{\mathbf{U}} \\ \mathbf{M}^{\circ} &= \mathbf{M} + \boldsymbol{\lambda}^{\circ} \\ \boldsymbol{\lambda}^{\circ} &= C_1\left[\mathbf{M} - \mathcal{A}\mathcal{Y}^{-1}\mathcal{A}^{\mathrm{T}}\right]. \end{aligned} \tag{9}$$

4 Good ansatz spaces

Efficiency of the proposed mass scaling technique significantly depends on the ansatz spaces for velocity [11]. The mass scaling works only if the ansatz space for velocity is poorer than the ansatz space for displacement. In order to provide high accuracy even for high values of scaling C_1, the ansatz should exactly represent all rigid body modes. Here for eight- and nine-node elements it is proposed to use following time-independent basis functions

$$\boldsymbol{\psi}_{=} \left[\begin{array}{cccccc} 1 & 0 & X^h & 0 & Y^h & 0 \\ 0 & 1 & 0 & X^h & 0 & Y^h \end{array} \right], \tag{10}$$

with X^h and Y^h being the reference position of points in element. In this case the rotary inertia of individual elements is accurately approximated for moderate distortions of elements. In addition, the term $\frac{\mathrm{d}\boldsymbol{\lambda}^\circ}{\mathrm{d}t}\dot{\mathbf{U}}$ in (9) vanishes. Another advantage of the basis is that the mass augmentation is invariant under rotation of reference configuration. This also means that the mass augmentation works efficiently even after finite rotations in actual configuration, which makes the approach very attractive for non-linear structural problems where finite rotations occur often. Note, that efficiency of this basis was tested for 4-node quadrilateral element in [11] and it was found inapplicable for the element.

Alternatively a time-dependent basis may also be considered, which allows exact preservation of the rotary inertia of individual elements. It reads as follows

$$\boldsymbol{\psi}_{=} \left[\begin{array}{cccccc} 1 & 0 & x^h & 0 & y^h & 0 \\ 0 & 1 & 0 & x^h & 0 & y^h \end{array} \right], \tag{11}$$

with x^h and y^h being the actual positions of material points. This ansatz requires update of the mass augmentation $\boldsymbol{\lambda}^\circ$ each time-step, which increases overhead on SMS. This basis is not examined in the examples below because of space limitations.

5 EXAMPLES

Performance of the proposed formulation is evaluated on two examples. The first example is a standard eigenfrequency benchmark for a tapered membrane from NAFEMS. The second example is a transient dynamics of simplistic 2D model of arch bridge.

For these examples LMM is computed in two different ways. For nine-node quadrilateral element standard row sum lumping is applied. For eight-node quadrilateral element Hilton-Rock-Zienkiewicz method is used [5]. Standard displacement formulation is used for stiffness calculation. Both the mass and stiffness matrices are computed using 3x3 Gauss quadrature rules. Eigenvalue benchmark is computed in computer algebra program *Maple*. The transient example is computed using in-house finite element code *NumPro*. In both cases hardware double precision numbers are taken for floating point operations.

5.1 FV32 eigenfrequency benchmark

The eigenfrequency benchmark FV32 of NAFEMS [1] considers a modal problem for a tapered membrane. Geometry, mesh and material properties of the membrane are presented in Figure 1. Clamping $u_x = u_y = 0$ is imposed along the y-axis.

Results of the benchmark are presented in Figures 2 and Tables 1 and 2. The ratio of frequencies for initial and mass scaled systems have expected form, i.e. several lower modes are almost unaffected for the variational mass scaling. The algebraic mass scaling changes the lowest modes much more, see Table 1. However, for the same increase of critical time-step dt,

the variational mass scaling yields higher conditioning of the mass matrix. This means that the variational mass scaling is more accurate but expensive method.

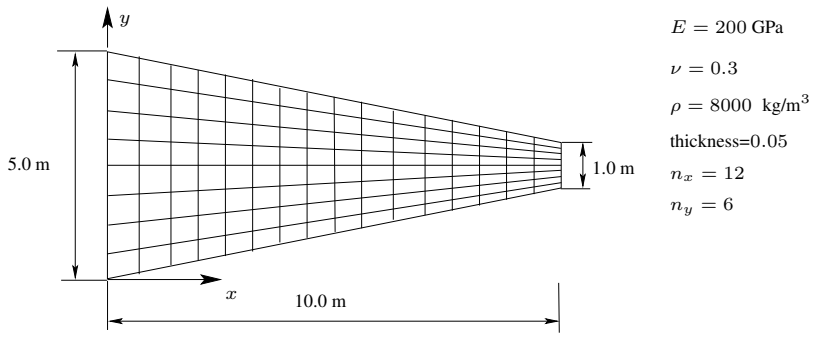

Figure 1: Setup of NAFEMS FV32 benchmark.

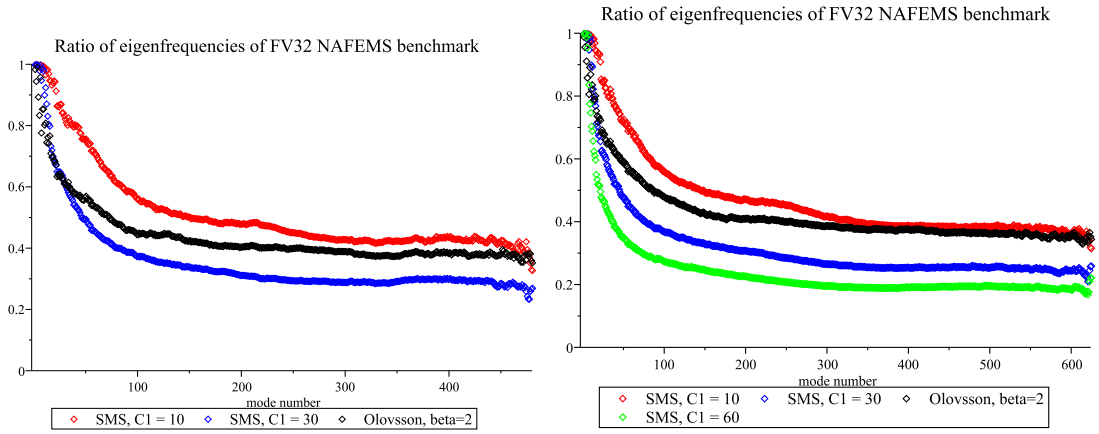

Figure 2: Ratio of eigenfrequencies for eight-node element (left) and nine-node element (right).

5.2 A model of an arch bridge

The model for a transient problem is shown in Figure 3. Initial zero displacements and velocities are assumed. The model is loaded in the middle of left arch by an abrupt point load F. Structural response is compared using history of the vertical displacement w under the load, Figures 4 and 5.

Computation with lumped mass matrices required 3691 and 2634 time-steps for eight- and nine-node element, respectively. For eight-node element following observations can be made. Application of small variational mass scaling factor $C_1 = 10$ with 1693 steps leads to very accurate results. Larger values of mass scaling result in larger conditioning of mass matrix without substantial reduction of time-step and are not recommended. Usage of algebraic mass scaling $\beta = 10$ with 832 steps increases inertia and results in phase shift of the displacement. For nine-node element similar behavior is observed. However, the conditioning of mass matrix for variational mass scaling is better.

The conditioning of mass matrix reflects on the number of necessary iterations for computation of the acceleration vector. The preconditioned conjugate gradient method with Jacobi

	f_1, [Hz]	f_1, [Hz]	f_3, [Hz]	f_4, [Hz]	f_5, [Hz]	f_6, [Hz]
reference	44.623	130.03	162.70	246.05	379.90	391.44
CMM	44.626	130.06	162.70	246.15	380.23	391.46
$C_1 = 10$	44.625	130.01	162.70	245.72	378.04	391.30
$C_1 = 30$	44.622	129.93	162.69	244.83	373.05	390.95
$C_1 = 60$	44.618	129.79	162.68	243.36	363.58	390.31
$\beta = 2$	43.943	122.99	161.50	220.18	317.47	375.50

Table 1: Six lowest eigenfrequencies f_{1-6} for FV32 benchmark with eight-node elements [1]

	eight-node		nine-node	
Mass type	dt_{crit}, [μs]	cond $\mathbf{M}$	dt_{crit}, [μs]	cond $\mathbf{M}$
LMM	8.7	49	8.4	79
CMM	14.8	219	13.4	128
$\beta = 10$	34.5	184	38.5	72
$\beta = 30$	50.1	236	64.8	153
$\beta = 60$	61.0	348	91.0	247
$C_1 = 30$	31.4	299	31.7	149
$C_1 = 60$	36.7	537	37.1	275
$C_1 = 100$	41.9	857	42.4	444

Table 2: Critical time-step and conditioning of mass matrix for FV32 benchmark

preconditioner is used for the numerical experiments. The relative error of residual norm is taken as 10^{-6}. For the nine-node element with values of algebraic mass scaling factor $\beta = 10$, 30 and 100, the average number of iterations is 25, 41 and 60, respectively. For values of variational mass scaling factors $C_1 = 30$, 100 and 300, the average number of iterations is 37, 65 and 111. This numbers perfectly correlate with the expected number of iterations, which is proportional to square root of condition number.

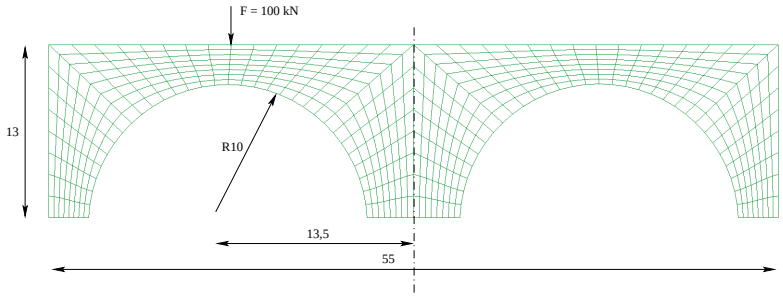

Figure 3: A model of an arch bridge. Material properties: $E = 30$ GPa, $\nu = 0.2$, $\rho = 2400$ kg/m^3, plane stress, thickness $= 1$ m. Mesh: 512 elements (eight- or nine-node quadrilaterals). Load: point force $F = 100$ kN applied in the middle of left arch. Duration: $t_{\text{end}} = 0.1$ s.

It was found that critical time-step and conditioning of mass matrix grow with C_1, see Table 3. Least square fit of the data yields following approximated relations

$$\begin{aligned} \text{eight-node:} \quad & \frac{dt^{\circ}_{\text{crit}}}{dt_{\text{crit}}} \approx 1 + \frac{2}{3}\sqrt[4]{C_1} \quad \text{cond}\,\mathbf{M}^{\circ} \approx \text{cond}\,\mathbf{M}_{\text{CMM}} + 3C_1 \\ \text{nine-node:} \quad & \frac{dt^{\circ}_{\text{crit}}}{dt_{\text{crit}}} \approx 1 + \frac{2}{3}\sqrt[4]{C_1} \quad \text{cond}\,\mathbf{M}^{\circ} \approx \text{cond}\,\mathbf{M}_{\text{CMM}} + \frac{4}{3}C_1. \end{aligned} \tag{12}$$

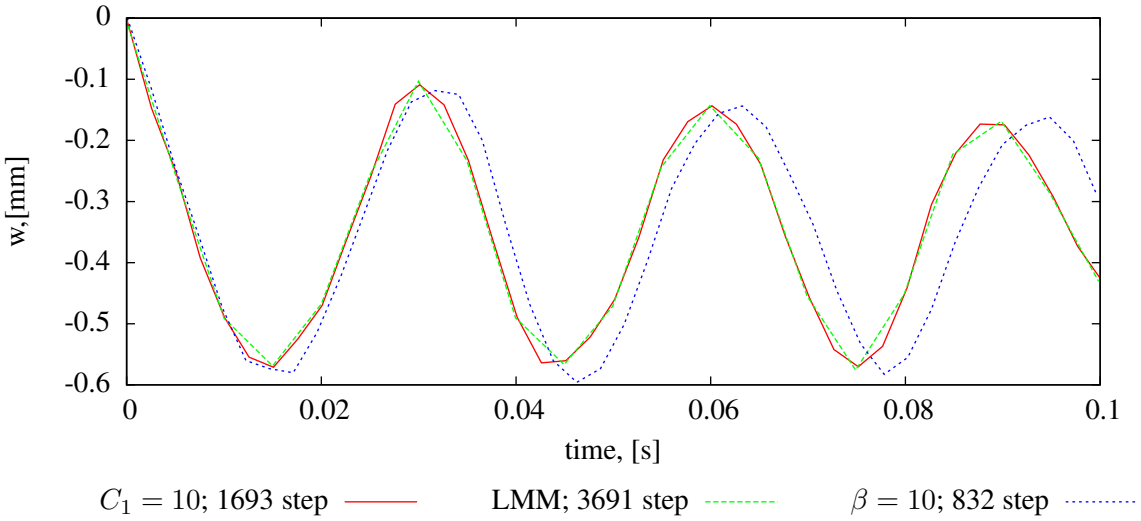

Figure 4: Displacement under external load. Results for eight-node element.

	eight-node		nine-node	
Mass type	dt_{crit}, [μs]	cond $\mathbf{M}$	dt_{crit}, [μs]	cond $\mathbf{M}^\circ$
LMM	26.8	19	42.0	29
CMM	42.4	93	26.5	62
$\beta = 10$	134.9	43	115.5	51
$\beta = 30$	227.1	98	194.5	115
$\beta = 100$	410.3	190	351.7	303
$C_1 = 30$	71.8	159	71.5	77
$C_1 = 100$	85.2	372	84.7	191
$C_1 = 300$	103.6	903	103.0	470

Table 3: Critical time-step and conditioning of mass matrix for the bridge model.

The quality of this fit is illustrated in Figure 6. On can see that rise of critical time-step is the same for eight- and nine-node elements. At the same time conditioning of scaled mass matrix $\mathbf{M}^\circ$ for eight-node element is much larger. Thus, it can prohibit its usage for large values of mass scaling C_1.

6 CONCLUSIONS

The main results of this contribution is extension of penalized Hamiltonian formulation to finite deformations with independent fields for displacement and velocity. Here it is proposed to use the new formulation for eight- and nine-node quadrilateral elements. Choice of ansatz spaces for velocity in form (10) allows an efficient implementation for selective mass scaling. This selective mass scaling works efficiently even after finite rotations.

The proposed mass scaling is tested for one eigenvalue and one transient benchmark. The eigenvalue benchmark showed better preservation of the lowest eigenfrequencies with the proposed method in comparison to algebraic mass scaling [10]. More accurate results with the proposed method are obtained for the transient benchmark. The phase error in oscillations is much lower. In addition the rules for growth of the conditioning of mass matrix $\operatorname{cond} \mathbf{M}^\circ$ and the critical time-step $dt^\circ_{\text{crit}}/dt_{\text{crit}}$ for discussed elements are found. This result can be used for

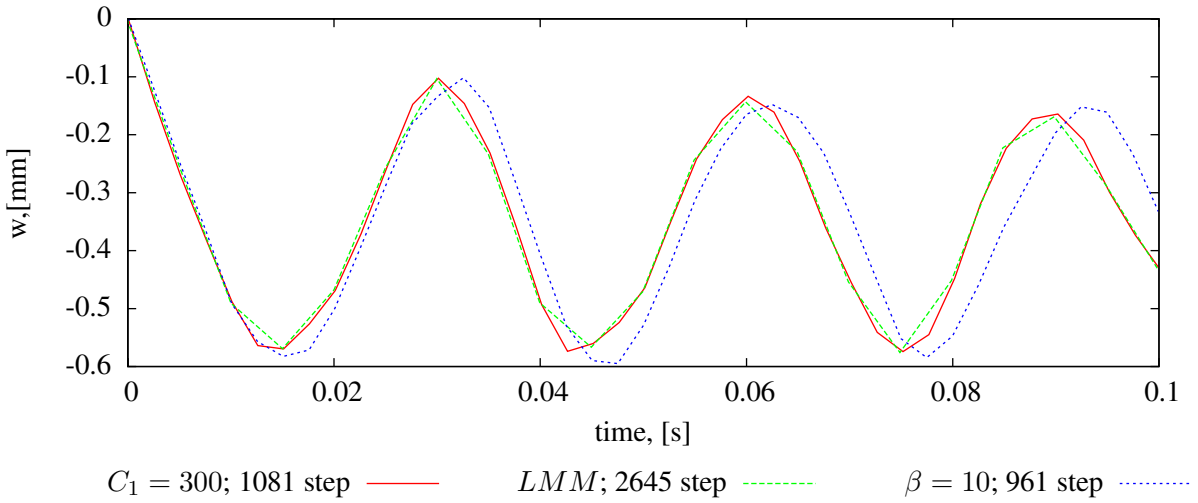

Figure 5: Displacement under external load. Results for nine-node element.

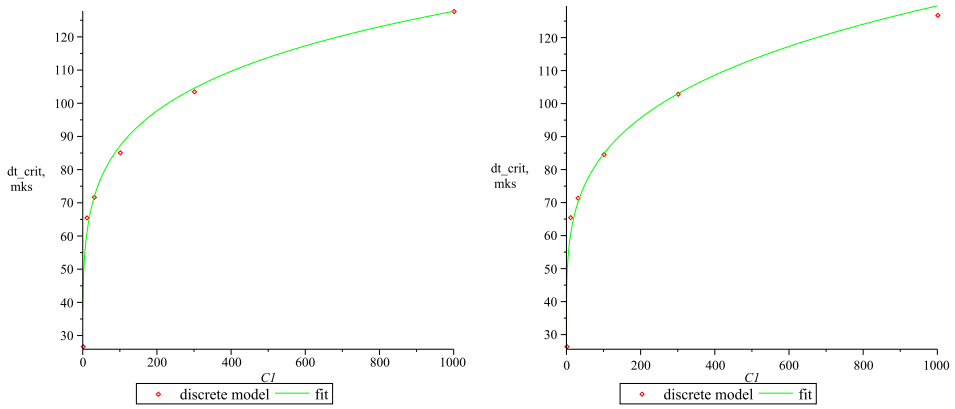

Figure 6: Dependence of the critical time-step on C_1 for eight-node (left) and nine-node (right) element. Computed values vs. fitted curve.

other structures for estimation of computational cost of selective mass scaling.

A possible directions of future work are extension of the variational mass scaling for 10-node tetrahedral elements, 20- and 27-node hexahedral elements and development of more efficient preconditioners for the scaled mass matrix.

The main conclusion is that variational selective mass scaling provides more accurate results than algebraic mass scaling. Application of variational selective mass scaling for quadratic elements reduce their computational cost in explicit codes and broad their usage.

Acknowledgements

Acknowledgements to Baden-Württemberg Stiftung gGmbH, Grant HPC-10, and Deutsche Forschungsgemeinschaft, Grant BI 722 7.1.

REFERENCES

[1] National Agency for Finite Element Methods & Standards (Great Britain). *The standard NAFEMS benchmarks*. NAFEMS, 1990.

[2] Ted Belytschko, W.K. Liu, and B. Moran. *Nonlinear finite elements for continua and structures*. Wiley, Chichester, 2000.

[3] T Borrval. Selective mass scaling in ls-dyna to reduce non-physical inertia effects. In *Developers' forum, DYNAMORE, Stuttgart, Germany, 2011*, 2011.

[4] Giuseppe Cocchetti, Mara Pagani, and Umberto Perego. Selective mass scaling and critical time-step estimate for explicit dynamics analyses with solid-shell elements. *Computers & Structures*, (0):–, 2012.

[5] E. Hinton, T. Rock, and O. C. Zienkiewicz. A note on mass lumping and related processes in the finite element method. *Earthquake Engineering & Structural Dynamics*, 4(3):245–249, 1976.

[6] S. W. Key and Z. E. Beisinger. The transient dynamic analysis of thin shells by the finite element method. In *Proc. of the Third Conference on Matrix Methods in Structural Mechanics*, 1971.

[7] R. Kolman, J. Plešek, D. Gabriel, and M. Okrouhlk. Optimization of lumping schemes for plane square quadratic finite element in elastodynamics. *Applied and Computational Mechanics*, 1:105 – 114.

[8] L. Olovsson, M. Unosson, and K. Simonsson. Selective mass scaling for thin walled structures modeled with tri-linear solid elements. *Comput Mech*, 34:134–136, 2004.

[9] Lars Olovsson and Kjell Simonsson. Iterative solution technique in selective mass scaling. *Comm Num Methods Engrg*, 22(1):77–82, 2006.

[10] Lars Olovsson, Kjell Simonsson, and Mattias Unosson. Selective mass scaling for explicit finite element analyses. *Int J Numer Methods Engrg*, 63(10):1436–1445, 2005.

[11] Anton Tkachuk and Manfred Bischoff. Variational methods for selective mass scaling. *Comput Mech*. in print.

[12] O.C. Zienkiewicz and R.L. Taylor. *The Finite Element Method Set*. Elsevier Science, 6 edition, 2006.